ELSEVIER

Journal of Hydrology 218 (1999) 169–190

Journal of Hydrology

The effect of vegetation on infiltration in shallow soils underlain by fissured bedrock

S.A. Stothoff[a,*], D. Or[b,1], D.P. Groeneveld[c,2], S.B. Jones[b,3]

[a]*Stothoff Environmental Modeling, Houston, TX 77006, USA*
[b]*Department of Plants, Soils, and Biometeorology, Utah State University, Logan, UT 84322-4820, USA*
[c]*Resource Management, Incorporation, Telluride, CO 81435, USA*

Received 26 March 1998; accepted 10 March 1999

Abstract

Mean annual infiltration above the high-level waste repository proposed to be sited at Yucca Mountain, Nevada, has a large impact on assessments of repository performance. Ongoing investigations of infiltration processes have identified the relatively horizontal caprock environment above portions of the repository as a potentially large source of infiltrating waters, due to shallow, permeable soils above a moderately welded tuff with large soil-filled fissures. The combination of shallow soils and fissured bedrock allows rapid penetration of wetting pulses to below the rooting zone. Plant uptake can strongly reduce net infiltration in arid environments with high water storage capacity, and, despite the low water storage capacity, there is a relatively high vegetation density in this environment. The apparent discrepancy between high vegetation density and low water storage motivates the study of plant-hydrologic interactions in this semiarid environment. Field observations were coupled with plant- and landscape-scale models to provide insight into plant-hydrologic interactions. Several lines of evidence, including: (i) linear plant growth features observed on aerial photographs; (ii) comparisons of plant cover within the fissured environment and comparable environments lacking fissures; and (iii) direct excavations, all suggest that the widely spaced soil-filled fissures are conducive to plant growth even when fissures are buried at soil depths exceeding 30 cm. Results from a mechanistic simulation model for root growth into fissures suggest that the additional (sheltered) plant-available soil water within fissures provides a competitive advantage for plant establishment. Therefore, plants that germinate above a fissure are more likely to survive, in turn developing linear features above fissures. Having established that plants preferentially root within soil-filled fissures in the caprock environment, a set of simulations were performed to examine the hydrologic consequence of plant roots within fissures at the landscape-scale. The response to three rainfall amounts was simulated. For the largest storm, fluxes at the fissure bottom peaked at 1–4 weeks after the storm when plant uptake was not active, but were eliminated when fissures had active vegetation. When plants were active within a fissure, uptake eliminated net infiltration in the fissure regardless of the size of the storm. Two plant-related mechanisms reduced total flux through the plant-filled fissures: (i) transpiration during fissure flow, and (ii) wetting-pulse retardation due to drier fissures prior to rain. The first mechanism appears to be dominant in these simulations. Results suggest that transpiration may strongly limit net infiltration (i.e. total deep

* Corresponding author. Present address: 1206 La Rue Street, 77019 Houston TX, USA. Fax: +1-713-520-9622.

E-mail addresses: stothoff@insync.net (S.A. Stothoff), dani@tal.agsci.usu.edu (D. Or), dgroen@csn.org (D.P. Groeneveld), sjones@mendel.usu.edu (S.B. Jones)

[1] Fax: +1-435-797-2637.

[2] Fax: +1-970-728-1708.

[3] Fax: +1-435-797-2117.

PII: S0022-1694(99)00038-4

percolation flux escaping the plant root zone); significant infiltration can occur, however, when plants are dormant, so that most infiltration would be expected to occur during winter.

Keywords: Infiltration; Transpiration; Fissure; Root uptake

1. Introduction

Yucca Mountain (YM), Nevada, is the potential site of a geologic repository for high-level radioactive waste. YM, located approximately 160 km northwest of Las Vegas, NV, comprises a sequence of fractured, welded and nonwelded tuffs, has an unsaturated zone up to 750 m thick, and has a mean annual precipitation (MAP) of 150–170 mm. YM is located within the transition zone between the Mojave Desert and the Great Basin Desert. The potential repository is currently designed to be located within a fractured, densely welded tuff layer approximately 250 m above the water table. Numerous assessments of the expected performance of the potential repository have identified the magnitude of deep percolation fluxes past the repository horizon as a critical factor in the potential-repository performance (Nuclear Regulatory Commission, 1994, 1995; Electric Power Research Institute, 1990, 1992, 1996; Eslinger et al., 1993; Sandia National Laboratories, 1992, 1994; Andrews et al., 1994; TRW, 1995). In turn, the magnitude of deep percolation fluxes is strongly dependent on the magnitude of net infiltration below the zone of evapotranspiration, providing strong motivation for studying and quantifying infiltration processes in the YM area.

Infiltration processes in the vicinity of YM have been examined in detail. Flint et al. (1994) present a conceptual model of shallow-infiltration processes at YM that is in general agreement with available data and modeling studies presented by Long and Childs (1993) and Stothoff (1997). The studies suggest that the mean annual infiltration (MAI) may be relatively high on ridgetops and sideslopes (due to accessible bedrock fractures), relatively low in deep alluvium (due to large soil–water storage capacity and plant uptake), and may be locally enhanced near ephemeral channels due to flow concentration. The trend toward greater MAI where shallow soils overlie fractured bedrock is suggested by disparate lines of evidence including geothermal heat-flux-anomaly analysis (Sass et al., 1988), bomb-pulse and natural tracers (Fabryka-Martin et al., 1996), and neutron-probe readings (Flint and Flint, 1995). If distributed recharge is significant at YM, with the aerial average of distributed recharge dominating the aerial average of concentrated recharge from ephemeral channels, recharge behaves somewhat differently than typically expected in arid and semiarid environments. This apparent anomaly provides motivation for studying flow processes in shallow soils (particularly in view of the sensitive response of potential-repository performance measures to net infiltration).

Deep recharge in arid and semiarid environments has been studied by various researchers, e.g. Allison and Hughes (1978), Allison et al. (1994), Barnes et al. (1994), Conrad (1993), Gee et al. (1994), Nichols (1987), Phillips (1994), Scanlon (1991, 1992) and Tyler and Walker (1994), and hydrologic interactions in deep soil profiles are reasonably well understood. Deep recharge is determined by the interaction of the spatial and temporal distributions of precipitation with evapotranspiration. Estimates of recharge in deep alluvium profiles near YM range from 8 to less than 0.01 mm/y (Tyler and Walker, 1994), corresponding to roughly 5 to less than 0.01% of the long-term average precipitation of 150 mm/y at the elevation studied. In the absence of vegetation, surface runon–runoff processes and bare-soil evaporation determine the fraction of precipitation resulting in net recharge. Where vegetation is present, plant water uptake may consume a large portion of the precipitation (Gee et al., 1994; Tyler and Walker, 1994).

Hydrologic interactions have been less examined in shallow soils underlain by fractured bedrock. Several studies are discussed by Sternberg et al. (1996). They note that in many mountainous sites with shallow soils, soil water storage is inadequate to support existing vegetation and several studies have found that roots of woody plants may penetrate many meters into bedrock along fracture planes and joints. In a field study with highly weathered bedrock, Sternberg

et al. (1996) found that the bedrock supplied nearly ten times as much water than did the soil, suggesting that weathered bedrock may form an important ecosystem component.

Approximately 60% of the ground surface above the potential repository footprint is characterized by fractured welded tuff, either exposed or overlain by soils (i.e. unconsolidated porous materials) generally less than 50 cm in depth. The tuff bedrock is relatively unweathered, with fractures and fissures exhibiting the most weathering. The low soil–water storage capacity and plentitude of fractures can result in rapid transmission of infiltrating waters to well below the top of the bedrock, as evidenced by rapid responses in neutron-probe data (Flint et al., 1994; Flint and Flint, 1995), and bomb-pulse ^{36}Cl hundreds of meters into the bedrock (Fabryka-Martin et al., 1996). Once within the fractured bedrock system, water would be expected to be minimally available for plant uptake. However, even with limited soil–water storage, there is well-established perennial (and annual) vegetation cover on these surfaces. In areas with exposed bedrock and very shallow soils (less than 10 cm), vegetation is easily found to be established in cracks and fissures. In areas with well-separated fissures and deeper soils (several tens of centimeters), vegetation often follows linear patterns suggestive of rooting into bedrock fissures. In soils unconstrained by bedrock and associated fissures, plant root density, and by analogy plant uptake, is commonly modeled as decaying approximately exponentially with depth (Gerwitz and Page, 1974; Campbell, 1985; Fayer and Jones, 1990). Plant root distributions and water uptake under the constraints of shallow soils and fissured bedrock have not been well established and are of direct interest for quantifying net shallow infiltration at YM.

Three general types of shallow-soil environments are predominant at YM: (i) the crystal-rich caprock environment, with widely spaced fissures, relatively verdant vegetation, and relatively shallow slopes; (ii) the crystal-poor welded-tuff environment, with frequent carbonate-filled cooling joints, relatively sparse vegetation, and relatively steep slopes; and (iii) the scree or talus environment, with no plants within the scree, relatively verdant vegetation bordering the scree, and slopes of 30–60%.

In this study, the caprock environment is examined in detail. As a result of relatively shallow slopes, the caprock environment is most accessible to field observation and may be the most amenable to modeling studies. Further, borehole and modeling studies (Flint and Flint, 1995; Fabryka-Martin et al., 1996; Long and Childs, 1993; Bagtzoglou et al., 1997) strongly suggest that MAI is relatively large within this environment. Little or no field data has been gathered in either of the relatively inaccessible sideslope environments to date, except at the extreme bottom and top of the slopes.

The overall objective of this study was to identify factors influencing hydrologic processes in the caprock environment using a combination of techniques. The specific objectives were to: (1) use aerial photography, coupled with field sampling, to (a) estimate vegetation composition and cover, and (b) identify linear vegetation patterns and examine potential attributability to subterranean fissures; (2) use a mechanistic root-growth simulation to test the hypothesis that rooting within fissures provide competitive advantage for plant establishment; and (3) investigate hydrologic interactions at landscape scale using two-dimensional (2D) modeling of water flow and uptake in mildly sloping caprock surface considering fissures and plants.

The article is organized as follows. Geologic setting, surficial deposits, and potential plant-fissure interactions are discussed in Section 2. Types of perennial vegetation present in the environment and field observations of rooting patterns in a linear feature are discussed in Section 3. Hypothesizing that the competitive advantage must be realized at the early stages of growth, a three-dimensional (3D) modeling exercise is described in Section 4 that simulates the growth of individual roots and soil–water uptake for a generic plant in the vicinity of a single fissure. Finally, a 2D modeling approach considering transpiration, lateral flow, and several fissures on a landscape scale is presented in Section 5, and the impact of vegetation on net infiltration for typical rainfall events is examined. Conclusions from the study are discussed in Section 6. The study is intended to ultimately provide input to modeling exercises that assess the performance of the potential repository.

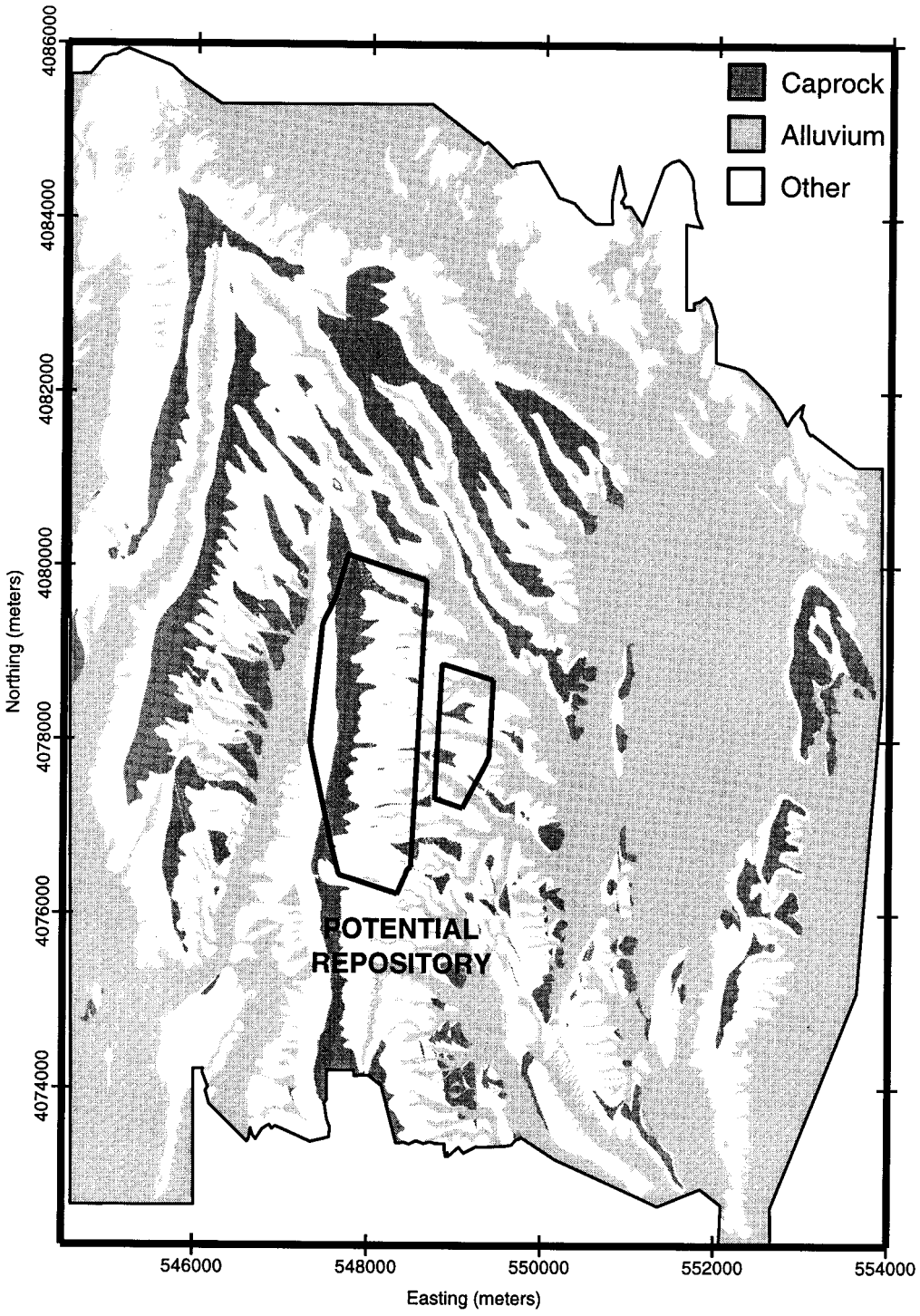

Fig. 1. Location of potential repository footprint at Yucca Mountain, NV, in UTM coordinates. Dark gray is caprock tuff, white is all other tuff, and medium gray is alluvium.

2. Background

2.1. Geologic setting

The proposed repository, shown in Fig. 1, is currently designed to be located in fractured, densely welded tuff approximately 250 m above the water table. The repository footprint, with an area of approximately 5 km^2, features 500–700 m of welded and nonwelded tuff units dipping 5–10° to the east. The west face of YM was formed by the steeply dipping north-trending Solitario Canyon fault. Within the repository footprint east of Yucca Crest, the tuff sequence is deeply dissected by washes cut into the welded Tiva Canyon unit of the Paintbrush Formation. Alluvial deposits in the washes can be several meters deep within the footprint and tens to hundreds of meters deep within a few kilometers of YM. On sideslopes and ridgetops within the repository footprint, shallow surficial deposits (called soils herein for simplicity of nomenclature) cover the fractured and fissured bedrock to depths typically less than 50 cm. Scree and talus deposits occur on steep sideslopes and can extend to depths greater than 1 m.

Tiva Canyon tuff, comprising several units of moderately to densely welded tuff, forms the bulk of the outcrop bedrock atop the potential-repository footprint. The units can be grouped into crystal-rich and crystal-poor tuffs (Buesch et al., 1996). The crystal-rich units overlie the crystal-poor units and tend to form an erosion-resistant layer that we refer to generically as caprock. The crystal-rich units form relatively massive blocks, with few cooling joints within a block but soil-filled (near the ground surface) fissures between blocks. The crystal-poor units are less resistant to erosion due to numerous cooling joints (typically carbonate-filled near the soil-bedrock interface), tend to be dissected into relatively steep washes atop the potential-repository footprint, and are overlain by scree or talus on portions of the steeper slopes. The focus of the current investigation is on the hydrologic behavior of the crystal-rich caprock forming much of the ridgetop environments at YM, particularly aspects of the hydrologic behavior affected by vegetation growing within the soil-filled fissures. Areas where crystal-rich Tiva Canyon units crop out are indicated by dark shading in Fig. 1.

Flint et al. (1996b) report typical saturated hydraulic conductivity values, based on 83 outcrop samples, of about 10^{-3} cm h^{-1} for bedrock units that we consider as lying within the caprock environment. Core samples from boreholes penetrating the same units suggest that bedrock in this environment may have two sets of values, with means on the order of 10^{-2} cm h^{-1} and 5×10^{-7} cm h^{-1} (Flint, 1996). For comparison, the densely welded crystal-poor units tend to have saturated hydraulic conductivities in the range of 10^{-4}–10^{-6} cm h^{-1} (Flint, 1996).

2.2. Surficial deposits and fracture fillings

The mildly sloping caprock surface is overlain by loamy sand soil of variable thickness, from exposed caprock to depths of about 0.5 m. Soil texture varies with depth from loamy sand to loam, typically features a light desert pavement at the surface, and exhibits occasional embedded rock shards and fragments at all depths. The fine-content composition (<2 mm) is remarkably spatially uniform on YM. Schmidt (1989) reports sand, silt, and clay contents of 60.8, 26.1, and 13.2 wt.%, respectively, and corresponding standard deviations of 5.38, 5.18, and 4.66%. Schmidt (1989) found that the gravel component (<75 mm) of the soil is 45.1 wt.%, with a standard deviation of 9.63. Our limited confirmatory analyses show average sand, silt, and clay contents of 66.4, 24.3, and 9.3 wt.%, respectively, with corresponding standard deviations of 5.29, 3.73, and 2.99, and electrical conductivity of about 0.4 mmho cm^{-1} for all 33 samples. Based on a soil texture analysis, Schmidt (1989) estimated the saturated hydraulic conductivity of the fine components to be about 2 cm h^{-1}. Several ponded-head permeameter measurements performed by the authors at scattered locations provided results consistently in the range of 10–18 cm h^{-1}. The Schmidt (1989) analysis included samples from the caprock, sideslopes, and alluvium-filled washes, while our analyses included only samples from caprock and sideslope environments.

Fine-textured fill, ranging from loam at the soil–rock interface to various forms of calcite (Quade and Cerling, 1990) at larger depths, is prevalent within fissures in crystal-rich Tiva Canyon caprock. Detailed analysis of the origin of the surface loamy sand soil and the sandy loam to loam filling the top portions of the fissures is beyond the scope of the study. However,

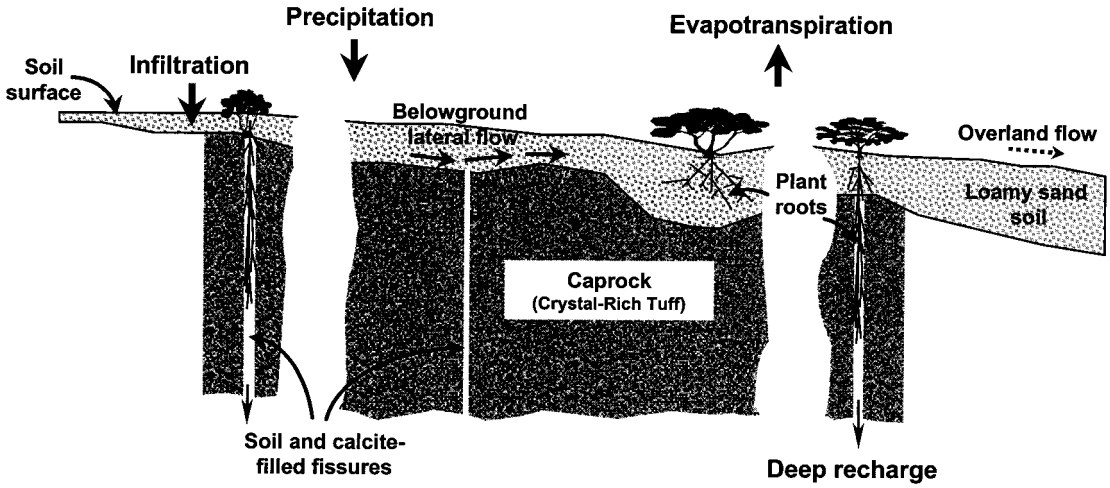

Fig. 2. Schematic of hydrologic features in the caprock.

based on the mineralogy and texture of these soils, their position in the landscape (top of the mountain crest), and the large loess deposits forming the fine component of the soils in Amargosa Valley and other nearby alluvial basins, these deposits are probably æolian. The uniform consistency of the fine components of the soils overlying various types of bedrock is the confirmatory evidence for an æolian origin. The source of the calcite is a matter of an ongoing debate; however, Quade and Cerling (1990) provide evidence that it is pedogenic.

2.3. Plant–fissure interactions

Plant–fissure interactions on Yucca Crest involve an array of hydrologic processes that are accentuated by the low storage capacity of the overlying soil, on the one hand, and focussed flows into and through fissures in the underlying bedrock, on the other. Other hydrologic processes also may occur, such as lateral flow at soil-bedrock interfaces and overland flow following heavy rainstorms. A schematic surface profile with the primary hydrologic processes under consideration is depicted in Fig. 2.

In water-limited ecosystems such as the YM area, it is thought that the vegetation density and patterns are controlled by the distribution and availability of soil water (Noy-Meir, 1973; Fonteyn and Mahall, 1981) and perhaps weathered-bedrock water (Sternberg et al., 1996). Stephenson, (1990) has shown that the (local) water balance is the single most important factor in explaining vegetation patterns in many ecosystems. Root growth into bedrock fissures has been studied in similar arid (Herwitz and Olsvig-Whittaker, 1989) and semiarid (Zwieniecki and Newton, 1995) ecosystems. Based on these studies, and on the polygon-like vegetation patterns on Yucca Crest (and similar nearby landscape units), we hypothesize that near-surface hydrologic processes interact with widely spaced fissures in the bedrock to provide conditions that enhance plant growth along the fissures. The role of vegetation in intercepting slowly moving water within fissures is of particular interest for deep recharge predictions at YM.

The fine-textured fill within fissures is a critical feature of plant–fissure interaction in crystal-rich Tiva Canyon caprock. Fine-textured fill not only helps in retaining a portion of the water feeding the fissure from above (thereby adding to the storage capacity available to roots), but also provides hydraulic continuity necessary for potential use of water held in bedrock pores (Zwieniecki and Newton, 1995). As evaporation takes place at much slower rates for deep fissures than from near-surface soil layers, soil–water storage in fissures can provide a means for survival of perennial vegetation during dry periods. Several caprock fissures are illustrated in Fig. 2. The left and right shrubs in Fig. 2 are the examples of plants dominated by interactions with fissures. There is

evidence, however, that widely spaced fissure-independent plants can also be established in relatively deep pockets of soil (center shrub in Fig. 2), with the shrub relying on the water-storage capacity of the soil.

Our hypothesis regarding the importance of fissures for supporting plant growth is supported by the disparity between relatively high vegetation density and low soil–water storage capacity in the caprock environment. Typical and extreme soil depths overlying the crystal-rich tuff are 0.2–0.6 m, respectively. Assuming the difference between field capacity and wilting point is 0.15 $m^3 m^{-3}$ (Ratliff et al., 1983), the plant-available soil–water storage capacities would be about 30–90 mm, respectively. Even when minimal transpiration rates of less than 0.1 mm/d are considered, the competing process of soil evaporation at relatively low rates of 1 mm/d (Evans et al., 1981) would have depleted the plant-available soil water from the 0.2 m soil profile within a month. Hence, we postulate that plants must rely on other, long-term soil water sources such as found in sediment-filled fissures in the caprock for areas with typical soil depths. The possibility of reliance on soil storage cannot be ruled out, however, in the deeper soil profiles of the caprock environment.

The lateral-flow processes shown in Fig. 2 are expected to be locally significant in the caprock environment, focussing water into fissures and drawing water toward plants. As a result of the relatively shallow slopes, prevalent bedrock fissuring, and numerous plants, it is anticipated that subsurface lateral flow rarely occurs over distances significantly larger than a few meters.

Overland flow in the YM caprock environment should be minimal. Soils at YM are sufficiently permeable, even if the hydraulic conductivity is as low as 2 cm h^{-1} as obtained from the texture analysis, that they should accept water at most rainfall rates until the wetting front contacts bedrock (a total influx of 3–9 cm for the soil depths discussed earlier). Overland flow may still be inhibited after the soil storage capacity is exceeded if soil water can quickly escape to depth within fissures. Overland flow would be expected to occur in areas with shallow-to-nonexistent soils, thereby concentrating the water into exposed fissures and downslope areas, but soils in the caprock area tend to deepen downslope (increasing storage capacity) so that the lateral extent of overland flow may be limited. In confirmation of these qualitative observations, geomorphic evidence for intense overland flow (such as erosive rills) is scarce in areas in which caprock is the bedrock material, although smaller amounts of overland flow may be present but masked by gravel armoring and reworking due to freeze–thaw processes.

3. Field investigation of vegetative patterns

3.1. Experimental methods

In approaching this study, we realized at the outset that the crystal-rich caprock provided a relatively favorable location for plant growth in comparison to locations downslope in which the tuff was less resistant. The caprock comprises relatively broad, gently sloping physiognomy that contrasts to the dissected arroyos comprising the stratigraphically deeper and less resistant tuff. Caprock-dominated environments exhibit occasional relatively deep (20–50 cm) pans filled with soil. These sites may perch water and, thus, foster greater vegetation cover than on locations of less resistant tuff that has similar aspect and slope and position just downslope and to the east of the caprock. The less resistant tuff generally has less soil cover as well (often 15 cm in depth or less). Perennial-vegetation measurements were obtained to document the relative richness of the caprock environment for vegetation. Annual species, which fluctuate greatly according to winter rainfall, were not recorded.

Vegetation was measured in the field at five locations on the crystal-rich tuff using the line point-quadrat technique (Heady et al., 1959). For this technique, sharpened pins were lowered vertically through the canopy at set intervals, using a 50 m tape stretched across the vegetation of interest. Contacts of the sharpened tips of pins (regarded as dimensionless (Goodall, 1952)) with the leaves of plants were recorded. Leaf area index (LAI), that is, the area of leaves per area of ground, was calculated by dividing total leaf contacts by the number of pins used on the transect, then multiplying by two to account for an extinction factor due to spherical leaf distribution (Groeneveld, 1997). Cover was calculated by dividing the total

Table 1
Average LAI and fraction cover of perennial plant species (nomenclature and authorities following Hickman (1995)) measured at five locations on slopes dominated by crystal-rich tuff. Affinity refers to species generally found in the Great Basin (G) or Mojave Desert (M)

Affinity	Species (Authority)	Family	LAI	Cover
G	*Eriogonum fasciculatum* (Benth.) Torrey & A. Gray	Polygonaceae	0.0745	0.068
G	*Grayia spinosa* Moq (Hook.)	Chenopodiaceae	0.145	0.064
G	*Ericameria cooperi* (A. Gray) H.M. Hall	Asteraceae	0.125	0.038
G	*Chrysothamnus teretifolius* (Durand & Hilg.) H.M. Hall	Asteraceae	0.063	0.030
G	*Ephedra nevadensis* S. Watson	Ephedraceae	0.039	0.028
M	*Lycium andersonii* A. Gray	Solanaceae	0.008	0.026
M	*Ephedra viridis* Cov.	Ephedraceae	0.027	0.018
M	*Hymenoclea salsola* A. Gray	Asteraceae	0.020	0.016
G	*Ericameria linearifolia* (DC.) Urb. & J. Wussow	Asteraceae	0.024	0.014
G	*Krascheninnikovia lanata* (Pursh) A.D.J. Meeuse & Smit	Chenopodiaceae	0.024	0.010
G	*Atriplex confertifolia* (Torrey & Fremont) S. Watson	Chenopodiaceae	0.0	0.008
G	*Atriplex canescens* (Pursh) Nutt.	Chenopodiaceae	0.0	0.006
G	*Achnatherum speciosum* (Trin. & Rupr.) Barkworth	Poaceae	0.0	0.004
		Total	0.549	0.330

number of pins that penetrated canopies, either hitting or missing leaves, by the total number of pins used on the transect. These transects were obtained on 26 and 30 March, 1997, prior to expected total leafout of the vegetation generally occurring during about mid-May (Leary, 1990).

Vegetation cover was also evaluated by photogrammetry on low-altitude, high-resolution vertical color-print air photographs of the repository block. For this analysis, approximately 30 m^2 homogeneous patches of vegetation on uniform slopes were chosen and overlaid with a template that delimited a grid field of 505 points. Perennial plant canopies underlying grid points were tallied. The frequency of these tallies versus the total number of grid points yields a measure of canopy cover equivalent to the total perennial vegetation cover measured by line-point transect; however, as a larger number of transects and concommitantly larger number of points can be obtained on the air photographs, the photogrammetric technique is statistically more robust. Hence, the line-point transects obtained in the field provide an estimate of species composition while the photogrammetric data were used to provide comparison between locations in which the hydrology was dominated by crystal-rich caprock and locations in which the substrate was derived from less resistant crystal-poor tuff.

3.2. Vegetation cover and composition

The perennial vegetation of the crystal-rich caprock tuff on YM is transitional between Great Basin and Mojavean flora but is dominated by species more typical of the Great Basin (Table 1). The measurements were obtained during late March, well in advance of the expected peak seasonal LAI; therefore, the overall observed LAI of 0.549 is probably less than the peak. In contrast, the cover developed in the field would not be expected to change through the season as the perennial plant canopies are persistent.

Table 2 presents the results from air photo interpretation of vegetation cover on crystal-rich caprock compared to locations on crystal-poor tuff that include ridgelines and north- and south-facing slopes. Aspect is an important predictor of vegetation cover on steeper slopes at YM; north- and south-facing aspects of the crystal-poor tuff have significantly different vegetation cover. This different cover is probably the result

Table 2
Mean perennial plant cover on Yucca Mountain, NV, measured on high-resolution air photos

Landscape position	Rock type	No. samples	Cover (STD[a])
Crest	Crystal-rich tuff	25	0.272 (0.066)
North aspects	Crystal-poor tuff	19	0.280 (0.071)
South aspects	Crystal-poor tuff	19	0.107 (0.034)
Ridgelines	Crystal-poor tuff	8	0.143 (0.039)

[a] Standard deviation of estimated plant cover.

of increased evaporation on south-facing slopes due to greater insolation. North-facing slopes are dominated by the Great Basin species while south-facing slopes are dominated by Mojavean flora.

The crystal-poor ridgelines had approximately the same aspect and slope as the crystal-rich caprock and were found to support vegetative cover only slightly greater than the south-facing aspects. Significantly higher vegetation cover exists on the caprock-derived over the noncaprock-derived ridgelines, despite the similar aspect and slope. These data indicate the promotional effect of the increased soil accumulation and rooting volume in the caprock environment. In addition, soil-filled fissures in the caprock environment may provide significantly more plant-accessible water storage than the carbonate-filled cooling joints prevalent in the crystal-poor ridgelines.

3.3. Experimental evidence for plant–fissure interactions

Of particular interest are those situations in which the spacing between adjacent fissures is larger than the extent of a typical rooting zone and the soil cover is too shallow to provide sufficient soil–water storage for vegetation. These conditions are likely to be conducive to alignment of vegetation along fissures. Such linear-like vegetation features should be observable on aerial photographs. To test this hypothesis, we analyzed high-resolution air photographs and identified several prospective sites with linear-like vegetation alignment. One such site is depicted in Fig. 3. The soil was excavated at two locations between plants along a linear vegetation feature (Fig. 3(a)) to expose the bedrock, revealing a large fissure (0.05–0.15 m in aperture) aligned with the vegetation (Fig. 3(b) and (c)). As not all perennial vegetation on the crest lies within a linear or polygonal feature, other forms of adaptation must also be taking place, such as: (i) exploitation of fissures by lateral growth of roots into fissures (as discussed in Section 4); and (ii) exploitation of soil bowls, due to irregularities in the caprock surface, that provide sufficient soil–water storage for plant growth. A confirmation of the latter mechanism was obtained by excavation.

4. Simulations of root growth into fissures

4.1. Methods

The linearity of vegetation features is hypothesized to arise from competitive advantage in the early stages of plant growth, as plants cannot relocate once established. To investigate the establishment of vegetation in the presence of shallow soils and bedrock fissures, a 3D simulator was used that explicitly models individual roots, root uptake, and soil–water fluxes (version 2.0 of the root-growth simulator (Clausnitzer and Hopmans, 1993; Clausnitzer and Hopmans, 1994; Somma et al., 1997)). These detailed simulations are in part intended to examine the potential applicability of the discrete-root methodology in deriving root distributions for future use in more traditional distributed-root models.

A simple test case was used to examine the competitive advantage enjoyed by a seedling located over a soil-filled fissure. The soil is assumed to be uniformly 10 cm in depth, and the fissure is assumed to be 15 cm wide. To ease the computational burden of 3D simulations, symmetry is assumed both perpendicular and parallel to the fissure, so that only half of the fissure is simulated and all side boundaries are represented as no-flow planes. The seedling is germinated in an upper corner of the domain, as shown in Fig. 4, so that one-quarter of a seedling root system is

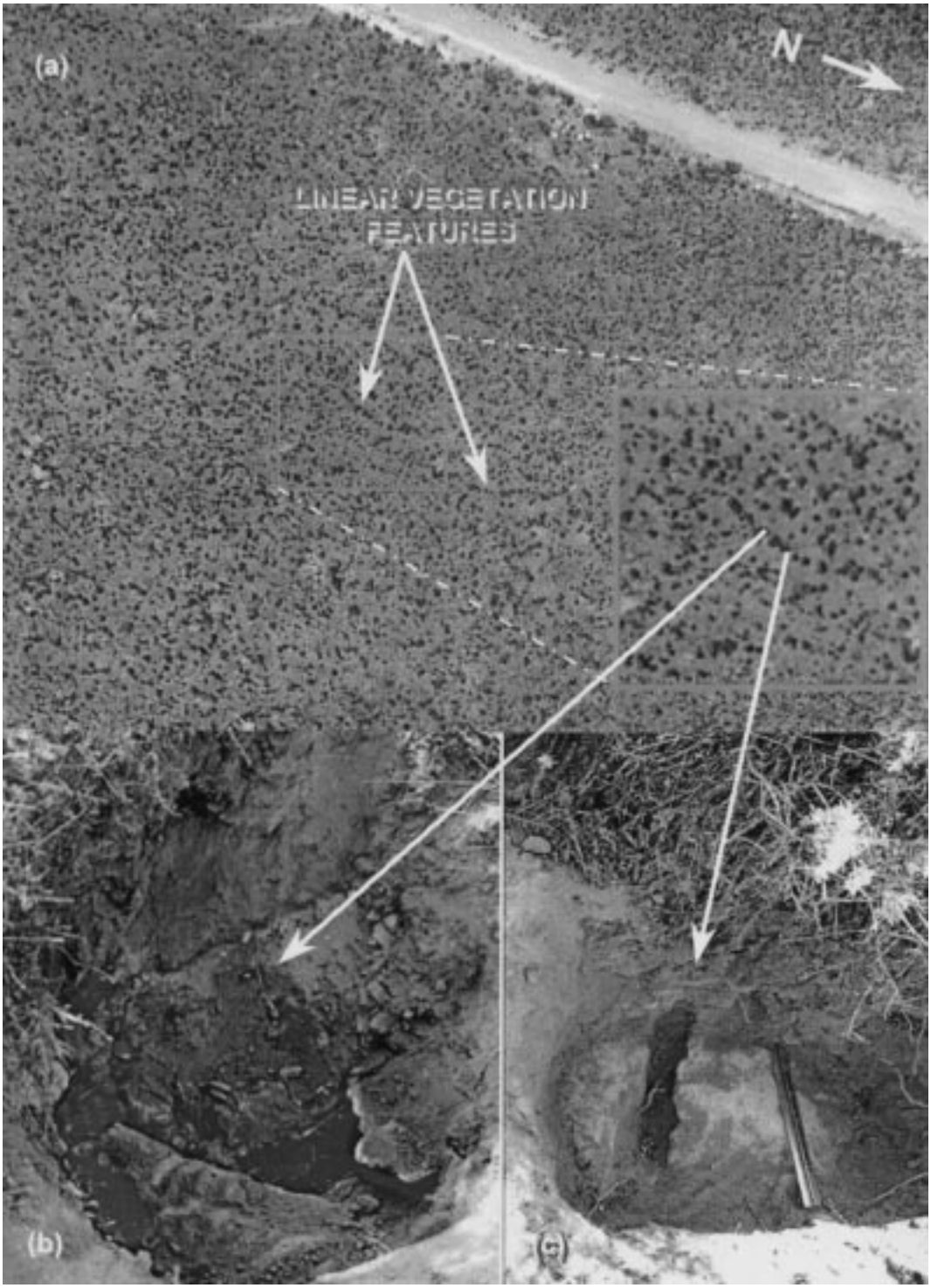

Fig. 3. Location of a linear vegetation feature in the caprock of Yucca Crest: (a) aerial view (roadway is approximately 3 m wide); (b) and (c) excavated fissures in bedrock.

represented for each simulation. In both cases, the seedling is located at the top of the soil layer; in case 1, the seedling is over the middle of the fissure, while in case 2, the seedling is over bedrock. In both cases, the seedling was given an initial leaf area of 2 cm^2 and a single main root, 1.73 cm long, extending diagonally into the domain. A computational grid consisting of elements 2.5 cm on a side was used, with total dimensions of $27.5 \times 25 \times 100\ cm^3$ for case 1 and $27.5 \times 25 \times 10\ cm^3$ for case 2. Residual saturation (θ_r), porosity (θ_{st}), van Genuchten α and n, and saturated hydraulic conductivity (K_{sat}) for both the soil and bedrock are reported in Table 3.

Number of parameters are required to describe the growth tendencies of a plant, many of which have not been measured for species of interest. Somma et al. (1997) provide estimated parameters that are reasonable for crop plants. In the interest of examining the growth characteristics of a generic plant to identify competitive advantage of fissure growth, most of the provided parameters were not changed, and neither nutrient nor temperature effects on growth were considered. The parameters that were changed were clearly unreasonable for vegetation adapted to water-stressed environments and were adjusted to achieve less water loss. The parameters used in the simulations are described in Table 4.

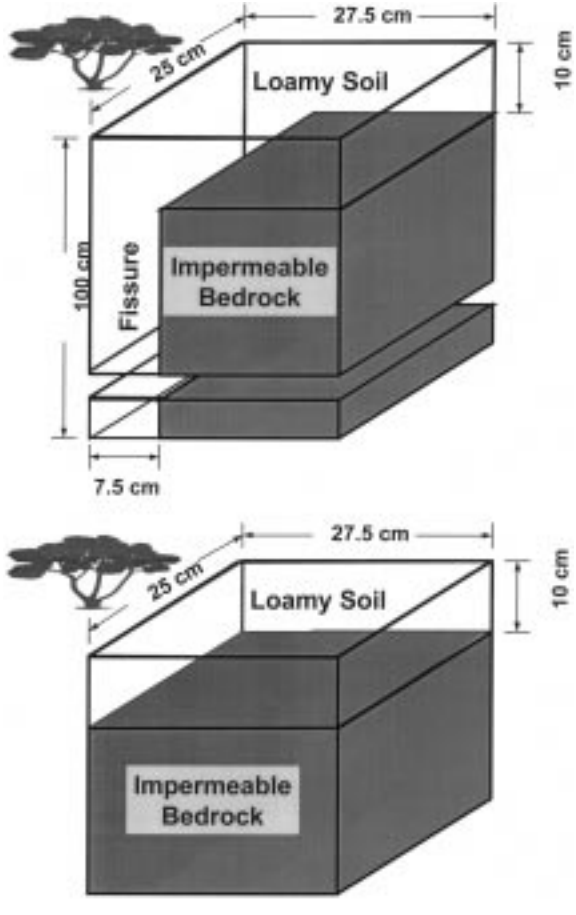

Fig. 4. Model domain for investigation of root growth: (a) fissured bedrock system, and (b) solid bedrock (no fissure exists).

Desert shrubs typically establish viable seedlings only during particularly favorable conditions. In the spirit of examining competitive advantages conveyed to a generic species, favorable conditions were imposed for growth. It was assumed that a thorough rainfall had uniformly brought soil suction head to 0.3 bar (300 cm suction) and bedrock suction head to 3 bar prior to the onset of growth. For 15 d, soil water was allowed to redistribute without evapotranspiration (a zero-flux condition for all boundaries), achieving substantially complete equilibrium between soil and bedrock. At the end of 15 d, the seedling was instantaneously emplaced, and the top boundary was transformed to a specified suction head of 5 bar (5000 cm) to simulate evaporation. All other boundaries remained zero-flux boundaries at all times. Small rainfall events were simulated at 15, 30, 45, and 75 d by instantaneously increasing the volumetric water content to 0.3 $m^3\ m^{-3}$ at every node in each column of nodes, starting with the top node in the column, until 7.5 mm of water was emplaced for each event. Each column of nodes was filled independently (i.e. lateral flow did not occur during filling).

4.2. Results

The root distributions resulting from the two simulations are superimposed in Fig. 5. In Fig. 5, the overall root system is shown from the direction perpendicular to the root system. An expanded view of the fissure-system roots is shown from above, and from the side parallel and perpendicular to the fissure, in Fig. 5(b)–(d)), respectively. Corresponding views of the impermeable bedrock system are shown in Fig. 5(e)–(g).

There is a significant difference between the mass of the two plants, with the plant over the fissure

Table 3
Hydraulic parameters for the porous media used in seedling simulation studies

Porous medium	θ_r ($m^3\ m^{-3}$)	θ_s ($m^3\ m^{-3}$)	α (m^{-1})	n (−)	K_{sat} ($m\ d^{-1}$)	Maximum strength[a]
Caprock[b]	0.002	0.105	0.049	1.43	2.4×10^{-9}	6
Loamy soil[c]	0.078	0.43	3.6	1.56	0.48	10^4

[a] Strength at residual saturation was arbitrarily selected, allowing growth in the soil with none in caprock.
[b] Retention parameters are for caprock sample PW19s (Flint et al., 1996b); K_{sat} was arbitrarily selected to be effectively impermeable.
[c] Retention parameters are for a loamy soil (Carsel and Parrish, 1988); estimated K_{sat} is for YM soil (Schmidt, 1989).

having total root and shoot dry masses of 0.278–0.308 g, respectively, while the plant over the bedrock has total root and shoot dry masses of 0.142–0.086 g, respectively. The plant germinating above the fissure is completely unimpeded by the rock and has extended roots 70 cm into the fissure. However, root growth for the plant above the bedrock is stunted; even lateral growth above the bedrock is inhibited.

Simulation of water uptake from a set of roots that have grown according to the environmental conditions has not been widely explored in the literature, particularly under the constraining conditions of bedrock. The observational study by Sternberg et al. (1996), particularly their Fig. 2, qualitatively supports the simulation results presented in this section, particularly the tendency for roots to follow fractures. The numerical simulation approach is quite time consuming, particularly as the mesh is refined and individual wetting events are considered. The code used for the simulations was designed for agricultural applications, thus the algorithms in the root-growth simulator are designed for soils with relatively smoothly varying strengths. The straightforward explicit algorithm used for growing roots, in which conditions at the root tip (e.g. soil strength, soil strength gradient) determine the size and direction of the root growth, can provide misleading results when there are strong gradients in soil strength such as at material interfaces. In such cases, the explicit algorithm can overshoot physical limits and place the root tip within the rock, where the root is trapped for all subsequent time steps. The simulator handles boundaries by reflecting any root tip crossing the boundary. The code was modified to handle rocks by using the same reflection approach to bypass the tip-growth algorithm whenever an element flagged as impermeable (i.e. rock) is encountered by a tip.

5. Landscape-scale hydrologic simulations

5.1. Methods

The HYDRUS-2D model (formerly known as SWMS-2D (Šimůnek et al., 1992)) was used to simulate the primary hydrologic processes at the landscape scale. The simulation domain represents a vertical 2D cross section (shown in Fig. 6) derived from the conceptual scheme shown in Fig. 2. Simulation domain dimensions, the finite-element mesh, and material locations are denoted in Fig. 6. The hydraulic properties for the four types of porous media considered are given in terms of van Genuchten parameters (van Genuchten, 1980) in Table 5. The simulation domain includes five vertical fissures in the caprock extending from the caprock surface to an underlying hypothetical fractured-tuff layer. The effective fissure aperture was set to 0.2 m (although 0.1 m may be more typical of the caprock) due to the relatively coarse resolution of the finite-element mesh imposed by computational constraints. There is minimal field evidence supporting the assumption that calcite is present in the bottom of the fissures. To examine the role of soil storage capacity, the soil cover increases from upslope to downslope. Fissure 1 represents a scenario in which precipitation falling on exposed bedrock is funnelled into downslope fissures, fissure 5 represents a moderately deep soil cover, and the remaining fissures represent intermediate scenarios.

To compare hydrologic fluxes within fissures with and without plant uptake, plants were placed over and within selected fissures in half of the simulations. Relative root distributions are depicted in Fig. 6. The system response to different rainfall-event magnitudes was considered in sets of three simulations: (i) 100 mm, representing an extreme convective summer storm; (ii) 30 mm, representing an average summer

Table 4
Parameters describing plant and root growth used in root-growth simulations. Functions are linearly interpolated between extremes and held constant outside of specified ranges

Parameter	Function	Value		
Potential transpiration rate per leaf area ($cm^3\ cm^{-2}\ h^{-1}$)	Constant	0.01		
Dry mass gained per volume of H_2O transpired ($g\ g^{-1}$)	Constant	0.0067		
Leaf area increase per increase in dry shoot mass ($cm^2\ g^{-1}$)	Constant	50		
Root/shoot ratio = *f*(time)	0 d	0.6		
	15 d	2.0		
Relative stress = *f*(soil strength)	0 bar	0		
	15 bar	1		
Transpiration multiplier = *f*(relative stress)	0	0.96		
	1	0.125		
Root/shoot ratio multiplier = *f*(relative stress)	0	1		
	1	1.2		
Roots starting at stem	Set 1	Set 2	Set 3	Set 4
Emergence Time (h)	0	24	120	240
Number emerging	1	2	2	2
Preferential growth relative to horizontal weighting factor	0.95	0.95	0.95	0.95
Maximum random deviation (°)	25	25	25	25
Branches	Order 1	Order 2	Order 3	
Unimpeded elongation rate (cm/h)	0.1	0.02	0.008	
Soil strength at which growth stops (–)	6	6	6	
Mass per unit length (gm/cm)				
Soil strength = 0	0.00030	0.00005	0.00001	
Soil strength = 6	0.00120	0.00020	0.00004	
Heading sensitivity to soil strength	0.1	0.5	1	
Maximum heading deviation per root time step (°)	45	45	45	
Maximum branch length (cm)	200	200	200	
Branch spacing (cm)	1	0.3	–	
Branching angle (°)	90	90	–	
Branching delay time at tip (h)	100	150	–	

thunderstorm; and (iii) 5 mm, representing the intensity and depth of an average winter storm. One set of three simulations was performed with no plant uptake; a second set considered plant uptake in fissures 2, 3, and 5. The first set of simulations is suggestive of winter conditions, with dormant vegetation, while the second set is suggestive of peak growing season. The boundary conditions for the simulations were: (i) free drainage at the downslope and bottom of the domain, (ii) no flux at the upslope side of the domain, and (iii) atmospheric boundary conditions on the soil surface. At the start of the simulation, a suction head of 500 cm (0.5 bar) was applied uniformly throughout the domain. For 4 d prior to the rainfall event, both potential-evaporation rates from the soil surface and potential-transpiration rates allocated over the depth of the roots were assumed to be 2 mm d^{-1}. The rainfall event took place uniformly over the duration of the fifth day. Subsequent to the rainfall event, the potential-evaporation rate was increased to 3 mm d^{-1}, and the potential-transpiration rate was increased to 4 mm d^{-1} for the reminder of the 35 d simulation.

5.2. Results

Among the six simulations are examples of each significant hydrologic process in the caprock environment under current climatic conditions. The only

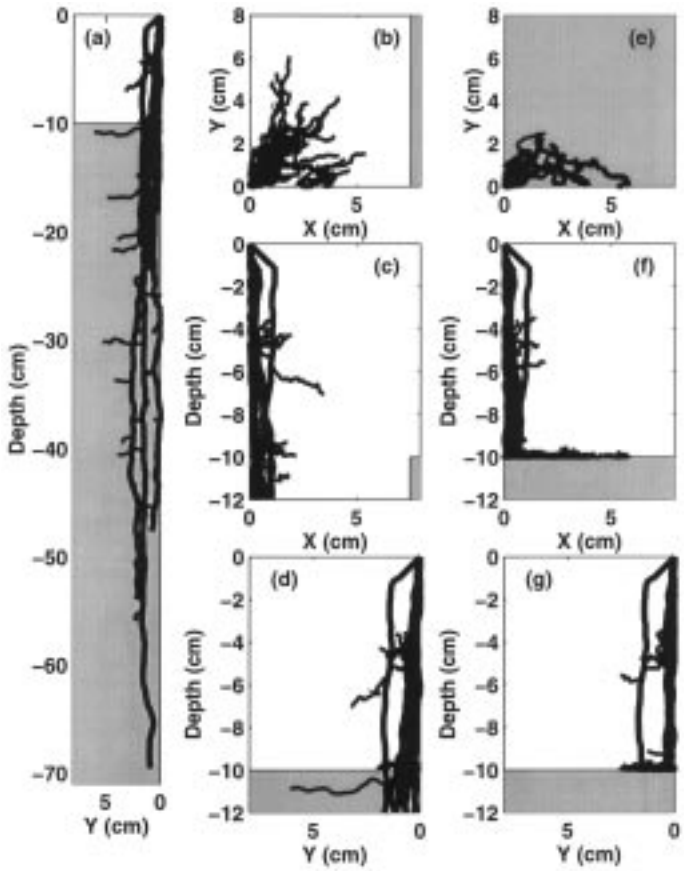

Fig. 5. Simulated root systems after 90 d of growth: (a) side view of the entire root system for the fissure simulation; (b)–(d) expanded views of the top of the root system for the fissure simulation, from the top, parallel to the fissure, and perpendicular to the fissure, respectively; (e)–(g) the entire root system for the solid-bedrock (no fissure) simulation from the same directions as in (b)–(d). Shaded areas represent bedrock while white areas denote soil.

potentially significant process not found is the relatively less important process of overland flow.

One method of assessing the impact of vegetation is to examine the cumulative flux in the fissures. For each of the five fissures, vertical fluxes at centerline nodes at the top of the fissure and at the top of the calcite were tracked. Downward fluxes are negative. For each of the 10 nodes and six simulations, the cumulative flux over the 30 d subsequent to the start of rainfall is shown in Table 6. The cumulative flux is reported across the soil–calcite interface in the fissures, at roughly the midpoint of the fracture length.

A comparison of cumulative fluxes between the same fissures with and without active plant uptake (fissures 2, 3, and 5 in Table 6) is strikingly suggestive of the potential for transpiring vegetation to reduce net infiltration in this fissured environment. For example, cumulative flux at calcite nodes is upward when active plants are in the fissure (i.e. plant uptake designated as ''yes'' in Table 6) and downward otherwise. Regardless of the size of the event, the same upward flux occurs. The vegetation has completely prevented the infiltrating water from affecting the calcite, and moreover is drawing water from the calcite. Cumulative downward flux tends to decrease even in fissures not containing plants, which can be attributed to lateral flow due to the presence of vegetation in adjacent fissures.

The 100 mm event represents the largest hydrologic perturbation to the system and would be most

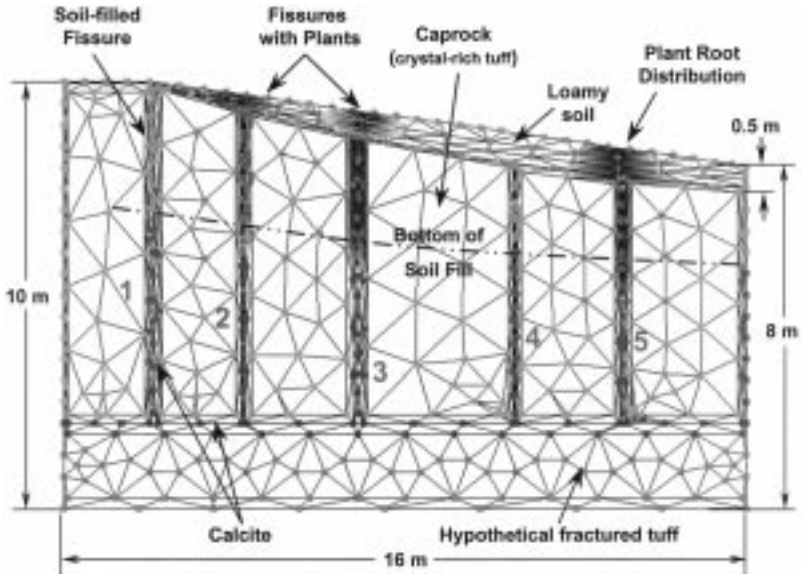

Fig. 6. Model domain for investigation of flow into fissures.

likely to result in net infiltration. For this event, the time history of fluxes within each fissure is shown in Fig. 7, with the same nodes presented in Table 6. The effects of lateral flow in the overlying soil upslope of fissure 1, focussing water into fissure 1, can be seen by noting that peak fluxes in Fig. 7(a) and (c) are one-third larger than the applied flux for several days after the precipitation event, while fluxes into the other fissures are significantly damped from the applied flux. The strong reduction of flow into those fissures with active plants can also be seen in Fig. 7(a) and (c), while the extraction of soil water from the calcite by plant uptake can be observed by comparison with Fig. 7(b) and (d).

The impact of plant uptake is even more marked in Fig. 8(a) and (c), which suggests that plants can completely shut off influx into fissures for moderate precipitation events. For this smaller event, the wetting pulse due to rainfall reaches a tiny peak at the calcite 3–4 weeks after precipitation when no plants are present (most of the flux is due to drainage of the initial conditions). The pulse is swamped by the impact of transpiration. As might be expected, the 5 mm event (not shown) shows no sign of a wetting pulse; evaporation in this system is sufficient to remove the wetting pulse before it reaches the fissure.

Moisture contents 9 d after the 30 mm wetting event are shown in Fig. 9, dramatically demonstrating

Table 5
Hydraulic parameters for the porous media used in landscape hydraulic simulation studies

Porous medium	θ_r ($m^3\,m^{-3}$)	θ_s ($m^3\,m^{-3}$)	α (m^{-1})	n (−)	K_{sat} ($m\,d^{-1}$)
Crystal-rich tuff (caprock)[a]	0.045	0.15	0.02	5.0	27×10^{-4}
Loamy soil[b]	0.078	0.43	3.6	1.56	3
Calcite (clay)[c]	0.05	0.20	0.8	1.09	0.048
Hypothetical fractured tuff	0.001	0.108	0.28	1.45	0.1

[a] Flint et al. (1996a).
[b] Retention parameters for a loamy soil (Carsel and Parrish, 1988) were used to emphasize the role of soil within the fissures (sandy loam to loam).
[c] Retention parameters for a clay (Carsel and Parrish, 1988) were used to emphasize the role of soil within the fissures (sandy loam to loam).

Table 6
Cumulative flux (mm) passing the soil–calcite interface in each fissure over the 30 d including and following the rainfall event. Negative values denote downward flux

Location	Event (mm)	Plant uptake	Fissure				
			1	2[a]	3[a]	4	5[a]
Top	100	No	−341	−226	−159	−153	−143
Top	100	Yes	−321	−25	−6	−93	−1
Top	30	No	−0.90	−1.43	−2.24	−2.26	−2.26
Top	30	Yes	−1.07	−0.02	−0.02	−1.57	−0.03
Top	5	No	0.83	0.15	−0.44	−0.81	−0.57
Top	5	Yes	0.63	−0.01	−0.02	−0.58	−0.03
Bottom	100	No	−18.2	−8.53	−47.1	−7.83	−10.8
Bottom	100	Yes	−14.6	0.91	0.03	−3.99	0.01
Bottom	30	No	−1.01	−0.94	−2.46	−0.97	−0.98
Bottom	30	Yes	−0.85	0.91	0.03	−0.72	0.01
Bottom	5	No	−0.91	−0.86	−2.20	−0.82	−0.80
Bottom	5	Yes	−0.81	0.91	0.03	−0.64	0.01

[a] Fissure with plant roots.

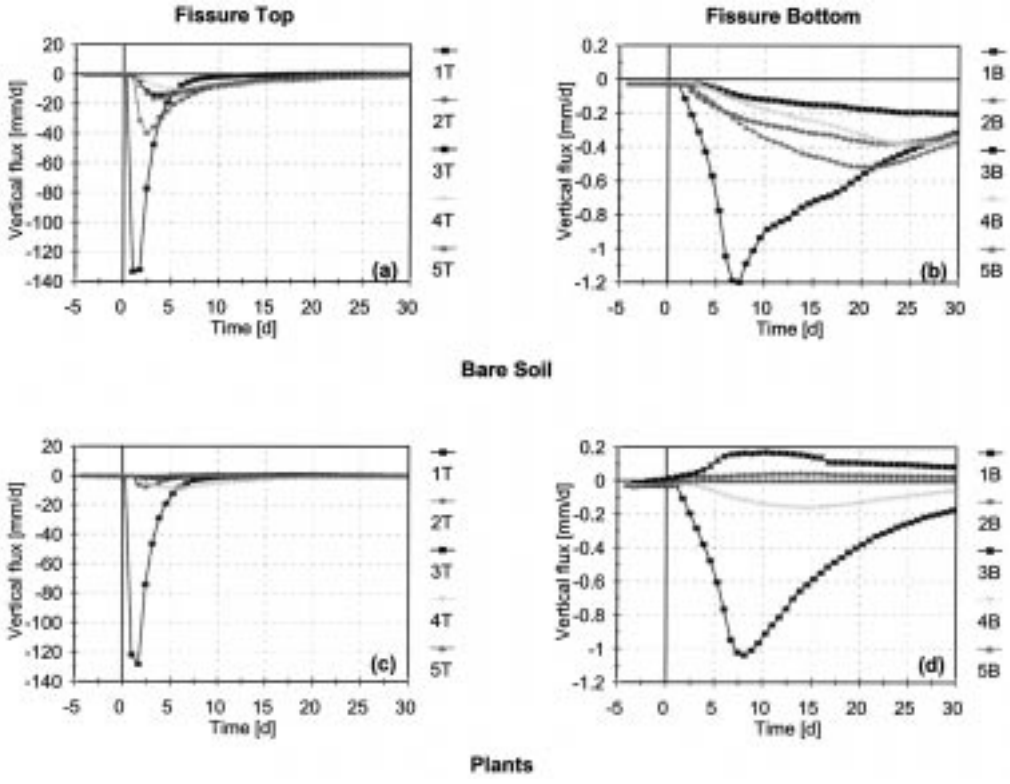

Fig. 7. Water flux in each of the five fissures following a 100 mm precipitation event: (a) and (b) top (T) and bottom (B) of soil-filled portion without plant uptake; (c) and (d) top (T) and bottom (B) of soil-filled portion with plant uptake.

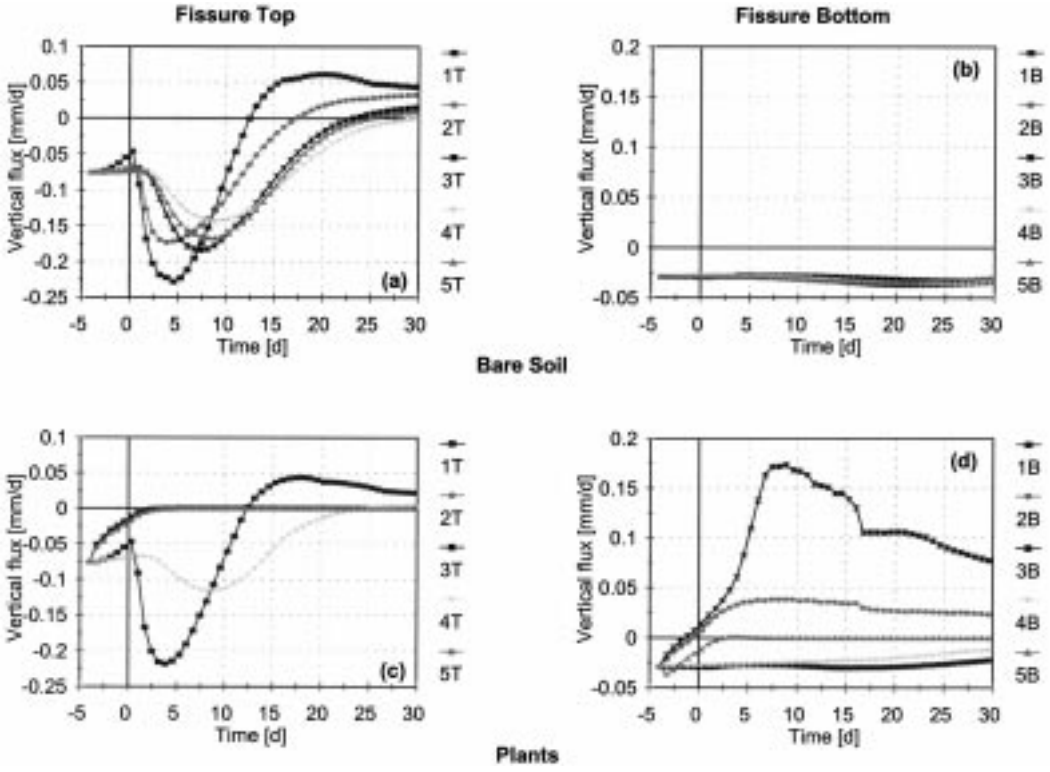

Fig. 8. Water flux in each of the five fissures following a 30 mm precipitation event: (a) and (b) top (T) and bottom (B) of soil-filled portion without plant uptake; (c) and (d) top (T) and bottom (B) of soil-filled portion with plant uptake.

a result of plant uptake. A small wetting front has penetrated the caprock by several tens of centimeters after 9 d without transpiration. With transpiration, the only caprock location with a wetting front is near the plant-free fissure 4, and the caprock has been dessicated near the plants. By drying the soil and bedrock matrix, plants can create hydraulic barriers in fissures and provide additional soil–water storage to intercept water fluxes.

The simulation results are qualitatively similar to field observations by Sternberg et al. (1996) in several field plots with shallow soil overlying highly weathered bedrock. Field plots containing native chaparral were compared with similar plots with the vegetation removed. As shown Sternberg et al. (1996) in their Fig. 3, the moisture content was considerably larger in the cleared plots by the end of typical growing seasons, even several meters below the ground surface. At 3 m depth, water contents in the vegetated plots did not respond every year, even though wetting pulses were observed each rainy season at shallower depths.

Plants dynamically regulate uptake, adjusting physiologic requirements to reflect the availability of soil water and seasonal cycles. Over time, plants can adjust their rooting distributions to provide efficient uptake during typical conditions near the plant during periods of active transpiration. Although the simulations presented here are suggestive of how transpiration is potentially able to dessicate the soil and bedrock, adaptive pressures may select plants that limit intake rates so that complete dessication is not achieved. Such adjustments are not simulated here, but simulations where MAI is of interest over long times may need to account for these adaptive processes.

In summary, having established that plants preferentially root within the soil-filled fissures in the caprock environment, a set of simulations were performed to examine the hydrologic consequence

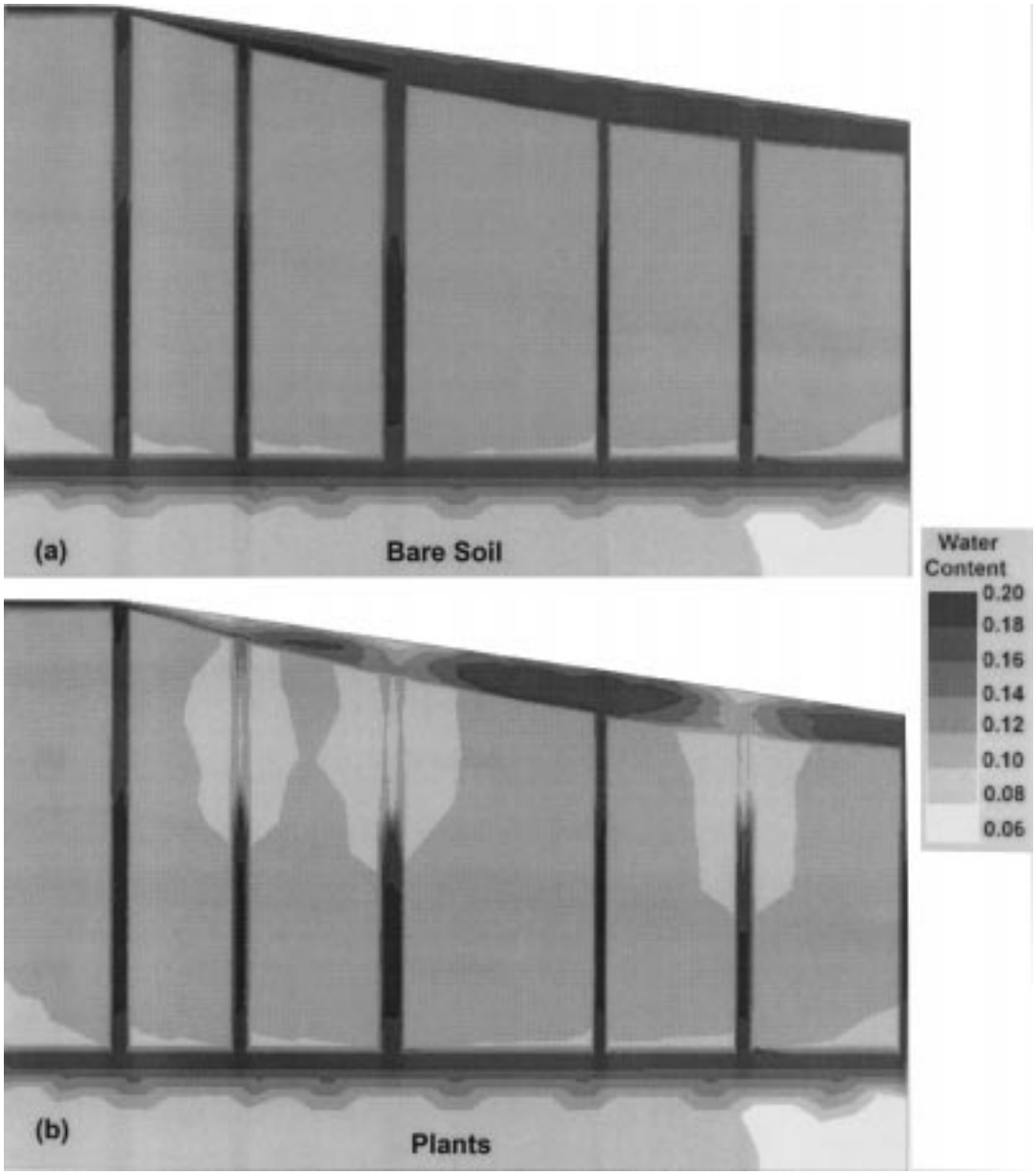

Fig. 9. Water-content distributions at the end of a 30 mm rainfall event: (a) without plants, and (b) with plants.

of plant roots within fissures. The response to precipitation was simulated for: (i) a shallow-soil-covered bedrock similar to the caprock environment, with three fissures containing plants and two fissures lacking plants; and (ii) an identical set of simulations completely lacking plants. The response to three rainfall amounts was simulated. For the largest storm, fluxes into the calcite filling peaked at 1–4 weeks after the storm when transpiration was not active and were eliminated when fissures had active vegetation. Smaller events enabled additional drainage from the initial conditions by providing additional soil water for evaporation. When plants were active within a fissure, transpiration eliminated net infiltration in the

fissure regardless of the size of the storm. Note that the efficacy of transpiration may be partly an artifact of the imposed transpiration rate, which (although reasonable) is not based on field measurements.

Two plant-related mechanisms reduced total flux through the plant-filled fissures: (i) uptake during fissure flow, and (ii) wetting-pulse retardation due to drier fissures prior to rain. The first mechanism appears to be dominant in these simulations. The set of simulations presented here demonstrate potential impacts of transpiration. The simulations suggest that net infiltration may be quite small in the caprock environment during the active growing season and exceptional circumstances (e.g. several large storms in a few days, vegetation die-off due to prolonged drought) may be required to cause net infiltration in this season. During the winter, when perennial vegetation is dormant (negligible transpiration), evaporation is minimal, and precipitation is relatively large, the simulations suggest that significant net infiltration can be more easily achieved. Accordingly, most infiltration would be expected during the winter.

6. Summary and conclusions

Several lines of investigation were used to examine the impact of vegetation upon hydrologic processes in a shallow soil overlying fissured bedrock. Field investigation of perennial vegetation reveals that Great Basin species tend to dominate Mojavean species in the caprock and upper sideslope areas of YM, both in the number of species present and in the total coverage (82% of the cover is due to Great Basin species). In general, Great Basin species tend to favor moister and cooler environments than Mojavean species. At YM, Mojavean species were found to dominate only on south-facing slopes with crystal-poor bedrock, which has vegetative cover of 44% of corresponding north-facing slopes and 48% of the crest (underlain by crystal-rich caprock). The crystal-rich caprock environment is more conducive to plant growth in general than environments underlain by the crystal-poor bedrock, as the vegetative cover in crystal-poor areas with the same general slope and aspect as the caprock environments is only 53% of the caprock cover.

Based on the field observations, the caprock environment is characterized by shallow loamy soils (0–60 cm in depth) having extremely uniform textures over the potential-repository footprint, widely spaced soil-filled bedrock fissures with apertures possessing widths on the order of 5–20 cm, and minimal carbonate deposition except perhaps at depth within the fissures and around rocks embedded within the soil matrix. Soil permeability is large enough to accept the water from most rainfall events without extensive runoff, which is corroborated by a general lack of field evidence for erosive rill formation.

The existence of linear vegetation patterns where the bedrock is covered by soil, readily apparent in low-altitude aerial photographs, is one of the striking features of the caprock environment. The exposed root structure of several perennial plants suggests that roots preferentially grow into bedrock fissures unless the soil–water storage capacity of a relatively deep pocket of soil can be exploited. Examination of the root structure for several aligned plants (selected from an aerial photograph) where soils are 30–60 cm deep revealed a bedrock fissure aligned with the plants, suggesting that the bedrock fissures provide a competitive advantage even when the overlying soils are fairly deep.

Hypothesizing that the environment the plant contacts during early growth exerts the primary control on plant distributions and that the environment atop a fissure is more conducive to plant establishment, a pair of simulations were performed that explicitly considered 3D soil–water redistribution, soil–water uptake by roots, and the growth of individual roots for a hypothetical plant during the early stages after germination. At the end of the 90 d simulation, the plant germinating above the fissure had twice the root mass and 3.6 times the shoot mass and leaf area than the plant germinating over bedrock, supporting the hypothesis. Interestingly, the plant germinating above bedrock was able to extract water from relatively permeable bedrock in simulations not shown here, suggesting that the bedrock may form a buffer for plants by storing water during moist conditions and slowly releasing the water over an extended period. Bedrock buffering is also supported by field observations that fine-root growth tends to be especially prolific immediately next to soil–rock interfaces, as also found by Zwieniecki and Newton (1995), and plant uptake from weathered bedrock

has been shown to dominate uptake from overlying shallow soils (Sternberg et al., 1996). Without bedrock buffering, it is difficult to provide a mechanism that enables the growth of lateral roots for long enough periods that a root can extend several meters across bedrock with overlying soil depths of only 5–10 cm, as we observed in the field for relatively slow-growing perennial shrubs.

Having established that the plants preferentially root within soil-filled fissures in the caprock environment, a set of simulations were performed to examine the hydrologic consequence of plant roots within fissures. The response to precipitation was simulated for: (i) a shallow-soil-covered bedrock similar to the caprock environment, with three fissures containing plants and two fissures lacking plants; and (ii) an identical set of simulations completely lacking plants. The response to three rainfall amounts was simulated. For the largest storm, fluxes into the calcite filling peaked at 1–4 weeks after the storm when transpiration was not active and were eliminated when fissures had active vegetation. Smaller events enabled additional drainage from the initial conditions by providing additional soil water for evaporation. When plants were active within a fissure, transpiration eliminated net infiltration in the fissure regardless of the size of the storm. The efficacy of transpiration may be partly an artifact of the imposed transpiration rate, which is not based on field measurements.

Two plant-related mechanisms reduced total flux through the plant-filled fissures: (i) transpiration during fissure flow, and (ii) wetting-pulse retardation due to drier fissures prior to rain. The first mechanism appears to be dominant in these simulations.

The impacts of neglecting transpiration and lateral flow were particular concerns raised by Stothoff (1997), who considered MAI for shallow soils over a fracture continuum under bare-soil conditions using one-dimensional (1D) simulations. Stothoff (1997) found that the simulated bare-soil MAI decreased roughly as a power of the soil depth when depths were shallow, qualitatively consistent with the results presented here for the 100 mm event without plants. The simulations presented by Stothoff (1997) tend to have most net infiltration occurring in the winter, with evaporation alone generally effective at eliminating net infiltration at other times. Although the simulations presented here were not designed to test the appropriateness of the 1D approximation, it appears that lateral flow rapidly equilibrates soil suction heads and lateral flow is relatively restricted. Accordingly, the use of 1D approximations may be justifiable in the caprock environment when vegetation is dormant.

The various lines of investigation discussed in this article suggest that the fissures have a dominant effect on recharge processes within the shallow-soil-covered caprock environment. Vegetation, dependent on soil–water availability, strongly shows the influence of fissures. Root-growth simulations suggest that the vegetation should have a strong preference for growing into fissures, and flow simulations also suggest that there should be strongly focussed flow into fissures. Despite the complexity of modeling this environment, several factors are conducive to relatively robust predictions of MAI. The caprock environment has long hiatuses between significant flow events triggered by the rare large precipitation events. During and immediately following such events, flow processes are characterized by a rapid time scale, large fluxes, rapid removal of water to below the rooting zone, and relatively low impact of vegetation during events that generate net infiltration. Deep alluvium also has long hiatuses between flow events, but due to relatively large soil storage subsurface flows are generally slower and it is more difficult for infiltrating water to move below the rooting zone. Thus, although flow processes in deep alluvium have been better characterized in the literature than in shallow soils, the relatively large and discrete net infiltration events in shallow soils may make predictions of MAI in shallow soils more robust than predictions in deep alluvium.

Acknowledgements

This article was prepared to document work performed by the Center for Nuclear Waste Regulatory Analyses (CNWRA) for the Nuclear Regulatory Commission (NRC) under Contract No. NRC-02-93-005. The activities reported here were performed on behalf of the NRC Office of Nuclear Material Safety and Safeguards, Division of Waste Management. The article is an independent product of the CNWRA and does not necessarily reflect the views or regulatory position of the NRC. The authors would like to

acknowledge the suggestions and comments made by G. Wittmeyer, B. Sagar, D. Woolhiser, and two anonymous reviewers, which tremendously improved the quality of the article.

CNWRA-generated data contained in this document have been documented according to quality assurance requirements described in the CNWRA Quality Assurance Manual. Sources for other data should be consulted for determining the level of quality for those data. Neither the HYDRUS-2D simulator nor the root-growth simulator is configured under the CNWRA's Software Configuration Procedure. At present, the CNWRA does not anticipate the use of either of these codes for regulatory reviews.

References

Allison, G.B., Gee, G.W., Tyler, S.W., 1994. Vadose-zone techniques for estimating ground-water recharge in arid and semiarid regions. Soil Science Society of America Journal 58 (1), 6–14.

Allison, G.B., Hughes, M.W., 1978. The use of environmental chloride and tritium to estimate total recharge to an unconfined aquifer. Australian Journal of Soil Research 16, 181–195.

Andrews, R.W., Dale, T.F., McNeish, J.A., 1994. Total System Performance Assessment-1993: An Evaluation of the Potential Yucca Mountain Repository. B00000000-01717-2200-00099-Rev.01, Intera, Incorporation Las Vegas, NV.

Bagtzoglou, A.C., Coleman, N.M., Pearcy, E.C., Stothoff, S.A., Wittmeyer, G.W., 1997. Unsaturated and saturated flow under isothermal conditions. In: Sagar, B. (Ed.), NRC High-Level Radioactive Waste Program FY96 Annual Progress Report, Volume NUREG/CR-6513, No. 1. Nuclear Regulatory Commission, Washington, DC, pp. 10-1–10-28.

Barnes, C.J., Jacobson, G., Smith, G.D., 1994. The distributed recharge mechanism in the Australian arid zone. Soil Science Society of America Journal 58 (1), 31–40.

Buesch, D.C., Spengler, R.W., Moyer, T.C., Geslin, J.K., 1996. Proposed Stratigraphic Nomenclature and Macroscopic Identification of Lithostratigraphic Units of the Paintbrush Group Exposed at Yucca Mountain, Nevada. Open-File Report 94-469, United States Geological Survey, Denver, CO.

Campbell, G.S., 1985. Soil Physics with BASIC. Elsevier, Amsterdam.

Carsel, R.F., Parrish, R.S., 1988. Developing joint probability distributions of soil water retention characteristics. Water Resources Research 24 (5), 755–769.

Clausnitzer, V., Hopmans, J.W., 1993. An Algorithm for Three-Dimensional, Simultaneous Modeling of Root Growth and Transient Soil Water Flow, V 1.0 LAWR Paper No. 100022, Department of Land, Air, and Water Resources, University of California, Davis, CA.

Clausnitzer, V., Hopmans, J.W., 1994. Simultaneous modeling of transient three-dimensional root growth and soil water flow adaptation. Plant and Soil 164, 299–314.

Conrad, S.H., 1993. Using environmental tracers to estimate recharge through an arid basin. Proceedings of the Fourth Annual High-Level Radioactive Waste Management Conference, American Nuclear Society, La Grange Park, IL pp. 132–137.

Demonstration of a Risk-Based Approach to High-Level Waste Repository Evaluation, 1990. EPRI NP-7057, Electric Power Research Institute, Palo Alto, CA.

Demonstration of a Risk-Based Approach to High-Level Waste Repository Evaluation, Phase 2, 1992. EPRI TR-100384, Electric Power Research Institute, Palo Alto, CA.

Yucca Mountain Total System Performance Assessment, Phase 3. EPRI TR-107191, Electric Power Research Institute, Palo Alto, CA.

Eslinger, P.W., Doremus, L.A., Engel, D.W., Miley, T.B., Murphy, M.T., Nichols, W.E., White, M.D., Langford, D.W., Ouderkirk, S.J., 1993 .Preliminary Total-System Analysis of a Potential High-Level Nuclear Waste Repository at Yucca Mountain. PNL-8444, Pacific Northwest Laboratory, Richland, WA.

Evans, D.D., Sammis, T.W., Cable, D.R., 1981. Actual evapotranspiration under desert conditions. In: Evans, D.D., Thames, J.L. (Eds.), Water in Desert Ecosystems. Dowden, Hutchinson, and Ross, INC. Stroudsburg, PA, pp. 195–218.

Fabryka-Martin, J.T., Turin, H.J., Wolfsberg, A.V., Brenner, D., Dixon, P.R., Musgrave, J.A., 1996. Summary Report of Chlorine-36 Studies. LA-CST-TIP-96-003, Los Alamos National Laboratory, Los Alamos, NM.

Fayer, M.J., Jones, T.L., 1990. unsat-h Version 2.0: Unsaturated Soil Water and Heat Flow Manual. PNL-6779, Pacific Northwest Laboratory, Richland, WA.

Flint, A.L., Hevesi, J.A., Flint, L.E., 1996a. Conceptual and Numerical Model of Infiltration for the Yucca Mountain Area, Nevada. Milestone 3GUI623M, Department of Energy, Las Vegas, NV.

Flint, L.E., 1996. Matrix Properties of Hydrogelogic Units at Yucca Mountain, Nevada. Milestone 3GUP604M, Department of Energy, Las Vegas, NV.

Flint, L.E., Flint, A.L., 1995. Shallow Infiltration Processes at Yucca Mountain, Nevada—Neutron Logging Data 1984–1993. Water-Resources Investigations Report 95-4035, United States Geological Survey, Denver, CO.

Flint, L.E., Flint, A.L., Hevesi, J.A., 1994. Shallow infiltration processes in arid watersheds at Yucca Mountain, Nevada. Proceedings of the Fifth Annual High-Level Radioactive Waste Management Conference, American Nuclear Society, La Grange Park, IL pp. 2315–2322.

Flint, L.E., Flint, A.L., Rautman, C.A., Istok, J.D., 1996b. Physical and Hydrologic Properties of Rock Outcrop Samples at Yucca Mountain, Nevada. Open-File Report 95-280, United States Geological Survey, Denver, CO.

Fonteyn, P.J., Mahall, B.E., 1981. An experimental analysis of structure in a desert plant community. Journal of Ecology 69, 883–896.

Gee, G.W., Wierenga, P.J., Andraski, B.J., Young, M.H., Fayer, M.J., Rockhold, M.L., 1994. Variations in water balance and recharge potential at three western desert sites. Soil Science Society of America Journal 58 (1), 63–72.

Gerwitz, A., Page, E.R., 1974. An empirical mathematical model to describe plant root systems. Journal of Applied Ecology 11, 773–782.

Goodall, D.W., 1952. Some considerations in the use of point quadrats for the analysis of vegetation. Australian Journal of Scientific Research 5, 1–41.

Groeneveld, D.P., 1997. Vertical point quadrat sampling and an extinction factor to calculate leaf area index. Journal of Arid Environments 36 (3), 475–485.

Heady, J.F., Gibbens, R.P., Powell, R.W., 1959. A comparison of the charting, line intercept and line-point methods of sampling shrub types of vegetation. Journal of Range Management 12, 180–188.

Herwitz, S.R., Olsvig-Whittaker, L., 1989. Preferential upslope growth of *Zygophyllum dumosum* Boiss. (Zygophyllaceae) roots into bedrock fissures in the northern Negev desert. Journal of Biogeography 16, 457–460.

Hickman, J.C., 1995. The Jepson manual of higher plants of California. University of California Press, Berkeley, CA.

Leary, K.D., 1990. Analysis of Techniques for Estimating Potential Recharge and Shallow Unsaturated Zone Water Balance Near Yucca Mountain, Nevada. PhD thesis, University of Nevada, Reno, NV.

Long, A., Childs, S.W., 1993. Rainfall and net infiltration probabilities for future climate conditions at Yucca Mountain. Proceedings of the Fourth Annual High-Level Radioactive Waste Management Conference, American Nuclear Society, La Grange Park, IL pp. 112–121.

Nichols, W.D., 1987. Geohydrology of the Unsaturated Zone at the Burial Site for Low-Level Radioactive Waste Near Beatty, Nye County, Nevada. Water-Supply Paper 2312, United States Geological Survey, Denver, CO.

Noy-Meir, I., 1973. Desert ecosystems: environment and producers. Annual Review of Ecological Systems 4, 25–52.

Initial Demonstration of the NRC's Capability to Conduct a Performance Assessment for a High-Level Waste Repository, 1992. NUREG-1327, Nuclear Regulatory Commission, Washington, DC.

NRC Iterative Performance Assessment Phase 2: Development of Capabilities for Review of a Performance Assessment for a High-Level Waste Repository, 1995. NUREG-1464, Nuclear Regulatory Commission, Washington, DC.

Phillips, F.M., 1994. Environmental tracers for water movement in desert soils of the American south–west. Soil Science Society of America Journal 58 (1), 15–24.

Quade, J., Cerling, T.E., 1990. Stable isotopic evidence for a pedogenic origin of carbonates in Trench 14 near Yucca Mountain, Nevada. Science 250, 1549–1552.

Ratliff, L.F., Ritchie, J.T., Cassel, D.K., 1983. Field-measured limits of soil water availability as related to laboratory-measured properties. Soil Science Society of America Journal 47, 770–775.

TSPA 1991. An Initial Total-System Performance Assessment for Yucca Mountain. SAND91-2795, Sandia National Laboratories, Albuquerque, NM.

Total-System Performance Assessment for Yucca Mountain-SNL Second Iteration (TSPA-1993), 1994. SAND93-2675, , Sandia National Laboratories, Albuquerque, NM.

Sass, J.H., Lachenbruch, A.H., Dudley, Jr., W.W., Priest, S.S., Munroe, R.J., 1988. Temperature, thermal conductivity, and heat flow near Yucca Mountain, Nevada: Some tectonic and hydrologic implications. Open-File Report 87-649, United States Geological Survey, Denver, CO.

Scanlon, B.R., 1991. Evaluation of moisture flux from chloride data in desert soils. Journal of Hydrology 128, 137–156.

Scanlon, B.R., 1992. Evaluation of liquid and vapor water flow in desert soils based on chlorine 36 and tritium tracers and nonisothermal flow simulations. Water Resources Research 28 (1), 285–297.

Schmidt, M.R., 1989. Classification of upland soils by geomorphic and physical properties affecting infiltration at Yucca Mountain, Nevada. Master's thesis, Colorado School of Mines, Golden, CO.

Šimůnek, J., Vogel, T., van Genuchten, M.T., 1992. The SWMS_2D code for simulating water flow and solute transport in two-dimensional variably saturated media V: 1.1. Research Report No. 126, US Salinity Laboratory, ARS USDA, Riverside, CA.

Somma, F., Clausnitzer, V., Hopmans, J.W., 1997. An Algorithm For Three-Dimensional, Simultaneous Modeling of Root Growth, Transient Soil Water Flow, and Solute Transport and Uptake, Version 2.1. lawr Paper No. 100034, Department of Land, Air, and Water Resources, University of California, Davis, CA.

Stephenson, N.L., 1990. Climate control of vegetation distribution: The role of the water balance. The American Naturalist 135, 649–670.

Sternberg, P.D., Anderson, M.A., Graham, R.C., Beyers, J.L., Rice, K.R., 1996. Root distribution and seasonal water status in weathered granitic bedrock under chapparal. Geoderma 72, 89–98.

Stothoff, S.A., 1997. Sensitivity of long-term bare soil infiltration simulations to hydraulic properties in an arid environment. Water Resources Research 33 (4), 547–558.

Total System Performance Assessment-1995. An Evaluation of the Potential Yucca Mountain Repository. B00000000-01717-2200-00136, TRW Environmental Safety Systems Inc., Las Vegas, NV.

Tyler, S.W., Walker, G.R., 1994. Root zone effects on tracer migration in arid zones. Soil Science Society of America Journal 58 (1), 25–31.

van Genuchten, M.T., 1980. A closed-form equation for predicting the hydraulic conductivity of unsaturated soils. Soil Science Society of America Journal 44, 892–898.

Zwieniecki, M.A., Newton, M., 1995. Roots growing into rock fissures: their morphological adaptation. Plant and Soil 172, 181–187.